CORPUS PUBLISHERS

Open Access Journal of Dental and Oral Surgery (OAJDOS)

Volume 2 Issue 3, 2021

Article Information

Received date: December 16, 2021

Published date: December 27, 2021

*Corresponding author

Solange de Paula Ramos, Research Group in tissue regeneration, Adaptation and repair, Department of Histology, State University of Londrina, Brazil

Research Article

Photobiomodulation Associated with Beta Tricalcium Phosphate Graft to Improve Initial Bone Healing

Roberta Gava Pratti[1], Avacir Casanova Andrello[2], Dari de Oliveira Toginho Filho[2], Wilson Trevisan Júnior[3] and Solange De Paula Ramos[1*]

[1]Research Group in tissue regeneration, Adaptation and repair, Department of Histology, State University of Londrina, Brazil

[2]Departament of Physics, State University of Londrina, Brazil

[3]Research Group in tissue regeneration, adaptation and repair, Department of Oral Medicine, State University of Londrina, Brazil

Abstract

Aim: Beta Tricalcium Phosphate (βTCP) is a synthetic bone substitute with osteoconductive properties, however, it is quickly reabsorbed, which can result in a smaller volume of newly formed bone. Light-emitting diode (LED) therapy has osteoinductive and anti-inflammatory properties, accelerates healing, and may improve the clinical performance of βTCP grafts. The work evaluated the effect of LED therapy (630 nm, 4J/cm^2) on βTCP grafts in the initial bone repair of bone defects in rat calvaria.

Methods: Forty-two male Wistar rats were randomly divided into two groups: Control and LED groups. In each animal, two perforations were made in the skull (4.3 mm diameter), one filled with βTCP (TCP) and the other with a blood clot (Co). Seven animals from each group were euthanized on the 7th, 14th, and 30th days and the samples were submitted to histological and microtomographic analysis.

Results: The Co-LED and TCP-LED defects presented increased defect areas and no inflammatory reaction after 7 days. After 14 days increased areas of primary bone were observed in the TCP and TCP-LED groups. After 30 days, TCP-LED defects presented reduced area and no foreign body reaction.

Conclusion: Phototherapy associated with βTCP accelerated the initial bone repair process compared to the isolated use of βTCP.

Keywords

Bone graft; Biomaterial; Bone matrix; Low-level light therapy

Introduction

Biomaterial grafts are synthetic material substitutes for the induction of bone regeneration. They are widely used in the treatment of periodontal disease, implantology, maxillary sinus lift, and alveolar ridge expansion [1-5]. Although autogenous bone grafts show good clinical performance, due to their osteoinductive and osteoconductive capacity, the morbidity (pain, bleeding, sensorial disturbances, bone defects) associated with the donor area is a limitation of the technique [6,7]. Among the alloplastic materials used as bone substitutes, clinical studies suggest that β-Tricalcium Phosphate (βTCP) can be used for the same purpose as autogenous grafts and in sinus lift grafting [1,8,9]. Studies have shown that βTCP is quickly reabsorbed, which may result in a smaller volume of the newly formed bone when compared to autogenous bone and bovine bone grafts [4,5,10,11]. Besides, βTCP may promote some undesirable reactions during the process of bone regeneration, such as the formation of fibrosis, chronic inflammation, and foreign body reactions, and may not reconstitute the entire bone volume [3,11-13]. The low osteoinductive capacity of βTCP makes the beginning of bone regeneration slower, compared to the bovine bone graft and autogenous graft [1,11,14]. To overcome this problem, other studies associated pure (monophasic) or biphasic (hydroxyapatite-associated) βTCP graft with insulin-like growth factor-1 and vascular endothelial growth factor [13], platelet-derived growth factor and recombinant bone-morphogenetic protein-2 [15], alendronate [3], stem cells derived from adipose tissue [10] and altering physical properties adding strontium-containing phosphate-based glass [16]. These procedures seem to improve the biological and physical characteristics of the βTCP graft, promoting osteoinductive activity, and increasing the volume of newly-formed bone tissue [2,4,13,17]. However, the addition of growth factors, cells, and physicochemical modifications of the βTCP particle may increase the cost of the production process or require additional laboratory treatment of the product.

Photobiomodulation using low-level lasers or light-emitting diodes (LED), has been used in the stimulation of bone tissue repair due to its anti-inflammatory and osteoinductive properties [18-20]. Photobiomodulation accelerates bone repair, and induces the differentiation and proliferation of osteoblasts, resulting in increased bone matrix formation [19,21]. The association of the osteoconductive capacity of βTCP and bone substitutes with the osteoinductive property of photobiomodulation could result in acceleration of the deposition of the primary bone matrix. An experimental study in rats demonstrated that phototherapy is capable of inducing the expression of bone morphogenetic growth factors such as bone morphogenetic proteins 1, 2, and 4 (BMP 1, 2, and 3), runt-related transcription factor-2 (RUNX-2), and transforming growth factor beta-1 (TGFß1) when applied in the first three days of bone repair [18]. Besides, the formation of primary bone began at the edges of the bone defect from the third day, being more advanced in animals submitted to phototherapy [18]. Considering the osteoinductive effects of photobiomodulation and osteoconductive effects of the βTCP graft, the objective of this study was to evaluate if the application of phototherapy in the first three days of bone repair can accelerate the initial deposition of primary bone in critical-sized defects in the calvaria of rats.

Material and methods

Animals

The procedures described in this study were approved by the Committee of Ethics in Animal Experimentation of the State University of Londrina (protocol n.24705/11). All procedures described herein conformed to the Ethical Principles for

Animal Research adopted by the Brazilian College of Animal Experimentation [COBEA; resolution 592 26/06/1992 of the Federal Council of Veterinary Medicine and law n. 9605 (regulated by Decree n. 3179, 21/12/1999)]. Forty-two male Wistar rats, approximately 300 grams, were obtained from the Animal Facilities of the State University of Londrina. The animals were housed in groups of 4 animals per cage, fed with normocaloric feed for rodents (Nuvilab, Nuvital company, Campo Largo, PR, Brazil) with free access to water. The temperature was maintained at approximately 25 ° C, in a light and dark cycle of 12 hours. The experimental design complied with the ARRIVE (Animal Research: Reporting of In Vivo Experiments) guideline.

Experimental Design

The animals were randomly divided into two groups of 21 animals, one being a Control group and the other undergoing photobiomodulation by light-emitting diode (LED) irradiation. In each animal, two perforations were performed in the skull, one randomly filled with βTCP graft and the other with a blood clot (Figure 1). Seven animals from each group were euthanized on days 7, 14, and 30. Bone defects were classified as:

Control group:

Co: bone defects filled with a blood clot.

TCP: bone defects filled with βTCP.

LED therapy group:

Co-LED: bone defects filled with a blood clot and treated with photobiomodulation.

TCP-LED: bone detects filled with βTCP and treated with photobiomodulation.

Surgical procedures

The animals were sedated and anesthetized with Ketamine hydrochloride solution (50mg/kg, Dopalen, Sespo Indústria e Comércio, Paulínea, SP, Brazil) and Xylazine hydrochloride (10mg/kg, Xilazin, Rhobifarma Indústria Farmacêutica, Hortolândia, SP, Brazil). Next, a surgical trichotomy was performed, the surgical area was cleaned with 2% iodinated solution and local anesthesia was applied with a solution of 1% Lidocaine hydrochloride with 1:200,000 epinephrine (Xylestesin, Cristália Produtos Químicos Farmacêuticos, Itapira, SP, Brazil) to avoid excessive bleeding during the surgical procedure. The linear coronal incision was made in the sagittal plane, with a scalpel blade n. 15, measuring about 1.5 cm in length. The periosteum was divulsed with a Molt periosteal elevator exposing the outer surface of the skull. Two bone perforations were performed in the parietal bones, preserving the cranial sutures and meninges with a low-speed trephine bur (Trefina 4.3 mm, Neodent, Curitiba, PR, Brazil), under refrigeration with sterile saline irrigation. The control defects were filled with a blood clot. The grafted defects were filled with βTCP graft (BetaPro, grain size: 150 to 500, Procell, São Carlos, SP, Brazil) (Figure 1a). The soft tissue was then sutured with a silk suture thread. Immediately after the surgical intervention, the animals received a single dose of procaine benzylpenicillin procaine and benzathine 10.000.000 IU and Dihydrostreptomycin 20g (Shotapen LA, Virbac, Carros, France) and an analgesic solution of sodium dipyrone (50 mg/kg, Febrax, Hertape Calier Saúde Animal, Juatuba, SP, Brazil), subcutaneously.

Photobiomodulation

Photobiomodulation was applied immediately after suturing, and 24, 48, and 72 h after surgery (Figure 1b) in 21 animals (Co-LED and TCP-LED bone defects). The LED probe (Bios Therapy II, Bios equipamentos médicos, São José dos Campos, SP, Brazil) was positioned in the operated area and the skull surface irradiated to deliver 6J of energy at a wavelength of 630nm. The LED probe presented an output power of 300mW, a power density of 200mW/cm^2, a spot area of 1.3 cm^2, and displayed an energy density of 4.6 J/cm^2, total energy of 6 J, during 20 s of irradiation. Seven animals from both the irradiated and non-irradiated groups were euthanized 7, 14, and 30 d after surgery by an intramuscular overdose injection of anesthetic solution. The skulls were immediately fixed in an aqueous Bouin solution for 24 h and stored in 70% alcohol before microtomographic and microscopic analysis.

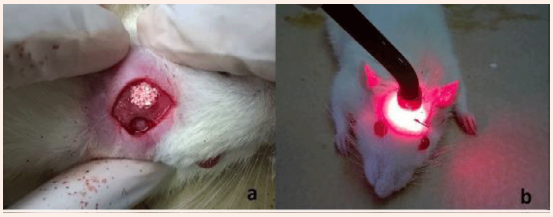

Figure 1: Beta-tricalcium phosphate graft and phototherapy. a) Two bone defects were made in the rat skull (parietal bones); one was filled with particulate βTCP and the other with a blood clot. b) After suturing, red light (630nm) phototherapy (4J/cm2) was applied using the optical tip of the Bios Therapy II equipment (Bios Equipamentos Médicos, São José dos Campos, Brazil).

Microtomographic analysis

Microtomography (micro-CT) was performed as described by Park (2007) [22]. The images were acquired in a Skyscan 1172 microtome (Bruker micro - CT, Kontich, Belgium) with a Hamamatsu 100/250 XR tube (Hamamatsu, Tokyo, Japan) with a voltage of 75 Kv and maximized power of 10W. A filter of 0.5mm was used for the acquisition of projections. For each sample, a micro - CT scanning was completed in an approximate sagittal plane through the anteroposterior profile of the skull, with a resolution of 8 μm and exposure time of 1000 ms. The micro-CT images were reconstructed using NRecon software version 1.6.4.7 (SkyScan, Kontich, Belgium), and performing corrections of artifacts. The software CTan version 1.11.9.1 (SkyScan, Kontich, Belgium) was used to select the region of interest (ROI), perform binarization of the image, and calculate the parameters of interest. Measured indexes determined the location and area of inorganic bone matrix deposition, the relative volume of graft material, relative soft tissue and hard tissue areas, the thickness of bone trabeculae, and bone density.

Histological analysis

After the micro-CT, the samples were decalcified in 50% formic acid solution, pH 1.5, and 20% sodium citrate, pH 7.9, for 30 d. The samples were included in paraffin and ten histological serial sections of 7μm, 70 μm apart from each other, were then stained with hematoxylin and eosin. The histological images were captured by optical microscopy in a Motican 2.0 image capture system (Motic, Xiamen, China) and analyzed in Motic Image Plus 2.0 software (Motic, Xiamen, China). The cross-sectional areas of the bone defect were analyzed for identification of the formation of primary bone, and the presence of inflammatory infiltrate and graft reabsorption. Microscopic images were analyzed by an experienced pathologist blinded to the defect treatment group.

Statistical analysis

Variables are expressed as mean (standard deviation) when the Shapiro-Wilk test indicated normal distribution of data. Differences between groups of defects were assessed using the ANOVA test, followed by the Tukey test (parametric data) or Student t-test. A difference between significant values was considered when $P < 0.05$. The mean number of animals per group was calculated based on the difference between the volume area of bone formation in critical-sized defects in rat calvaria after four weeks, analyzed by micro-CT images [23]. A total of seven animals were included, considering 20% of lost, to achieve a statistical power of 80% and a significant level of 5%.

Results

Microtomographic analysis

The microtomographic images demonstrated the particulate TCP graft-filled bone defects (Figure 2a) but in some areas the graft material extravasated beyond the edges of the bone defects (Figure 2b). Particulate TCP presented high radiopacity and was not resorbed until 30 d in the TCP and TCP-LED defects. After 7 d, the Co-LED and TCP-LED groups demonstrated an increase in the area of the bone defect, suggesting that the edges of the lesion had been reabsorbed (Figure 2c). However, after 14 d, the area of the defects in the Co-LED and TCP-LED groups was reduced in relation to the Co group and did not differ from the TCP group (Figure 2d). After 30 d, the TCP defects presented a smaller area than the Co and Co-LED groups, and the smallest defect area was observed in the TCP-LED group (Figure 2e). Analysis of the volume of the remaining TCP particles and the edges of the bone defects of the grafted groups (Figure 2a) suggests that photobiomodulation did not promote accelerated reabsorption of graft material and did not alter the porosity of primary bone tissue.

Histological Analysis

7 days

At 7 d, bone defects in all animals were filled with granulomatous tissue and presented a proliferation of periosteum remaining at the edges of the bone defects (Figure 3). In the Co group of bone defects, hemorrhagic areas close to the bone surface (Figure 3a) and the presence of chronic inflammatory infiltrate (mononuclear cells and few polymorphonuclear leukocytes) were observed. The central region of the defect was filled with granulomatous-looking tissue containing fibroblast-like cells, and a non-calcified

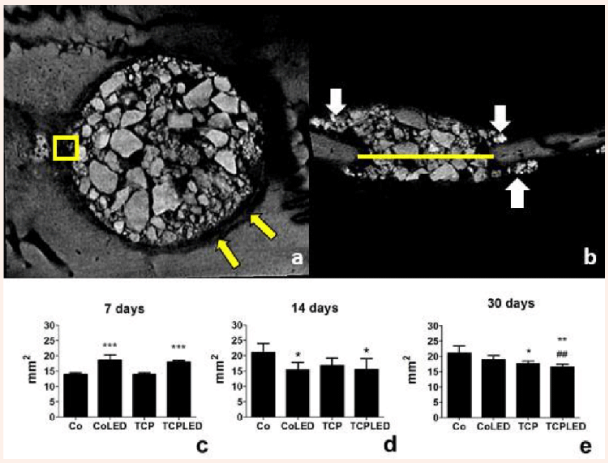

Figure 2: Microtomographic Analysis of bone defects. Bone surface (a) and transverse plane (b) of bone defect of the TCP-LED group after 30 days. (a) Radiopaque graft particles filled the bone defect. The yellow box indicates one ROI and the yellow arrows indicate areas with primary bone. (b) In the transverse section, extravasation of the graft material (white arrows) is observed over the internal and external periosteum region of the skull. The red line demonstrates the diameter measure considered to calculate defect areas. Area of bone defect at 7 days (c), 14 days (d), and 30 days (e). *** p <0.005, ** p <0.01 and * p <0.05 in relation to Co defects. ## p <0.01 in relation to the TCP, Tukey's test.

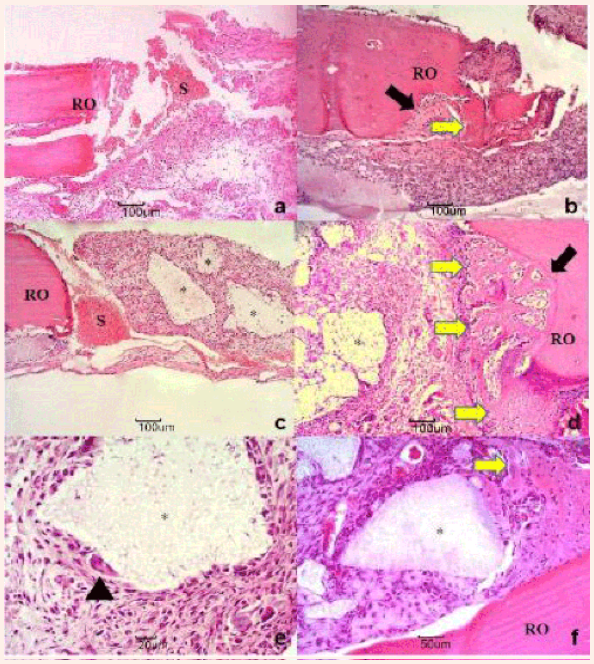

Figure 3: Microtomographic Analysis of bone defects. Bone surface (a) and transverse plane (b) of bone defect of the TCP-LED group after 30 days. (a) Radiopaque graft particles filled the bone defect. The yellow box indicates one ROI and the yellow arrows indicate areas with primary bone. (b) In the transverse section, extravasation of the graft material (white arrows) is observed over the internal and external periosteum region of the skull. The red line demonstrates the diameter measure considered to calculate defect areas. Area of bone defect at 7 days (c), 14 days (d), and 30 days (e). *** p <0.005, ** p <0.01 and * p <0.05 in relation to Co defects. ## p <0.01 in relation to the TCP, Tukey's test.

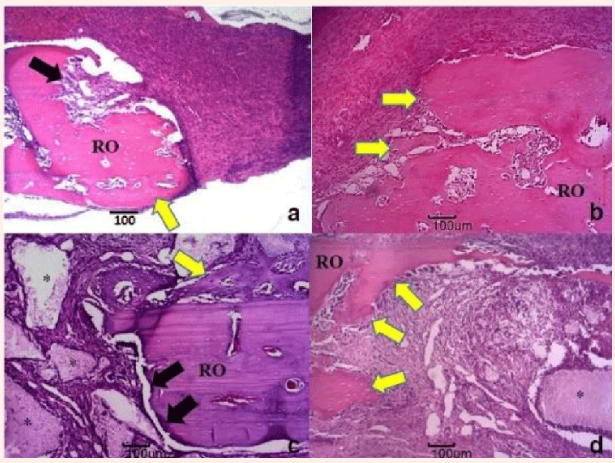

Figure 4: Histological images of bone defects in the skull of Wistar rats after 14 days. (a) Control (Co): bone defect filled with a blood clot. (b) Co-LED: bone defect filled with a blood clot and treated with photobiomodulation. (c) TCP: bone defect filled with βTCP. (d) TCP-LED: bone defect filled with βTCP bone graft and photobiomodulation. The black arrow indicates areas of bone resorption, the yellow arrow indicates areas of bone neoformation. RO: bony ridge; * BTCP particle. 40X, staining with Hematoxylin and Eosin.

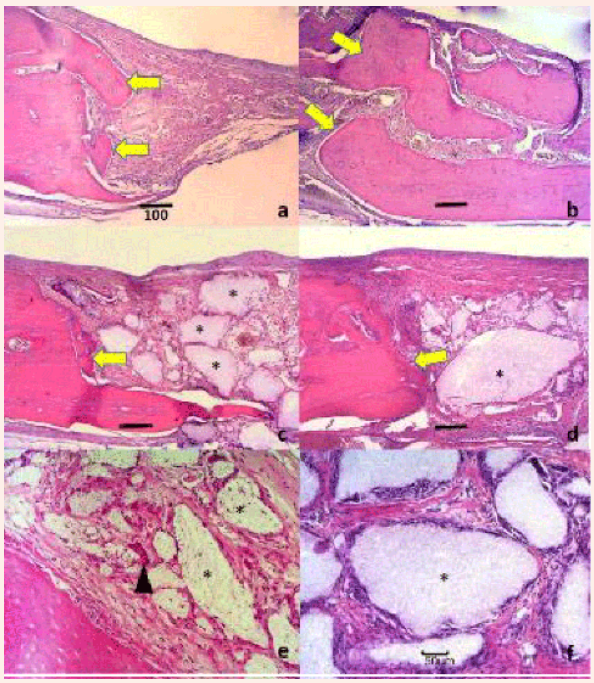

Figure 5: Histological images of bone defects in the skull of Wistar rats after 30 days. (a) Control (Co): bone defect filled with a blood clot. (b) CoLED: bone defect filled with a blood clot and treated with photobiomodulation. (c) TCP: bone defect filled with βTCP. (d) TCP-LED: bone defect filled with βTCP bone graft and photobiomodulation. (e) TCP, 200X. (f) TCP-LED, 100X. The yellow arrow indicates areas of bone neoformation. The arrowhead indicates a foreign body giant cell. RO: bony ridge; * BTCP particle. 40X, staining with Hematoxylin and Eosin.

matrix abundant in collagen fibers and blood vessels.

In the Co-LED bone defects, no areas of inflammatory infiltrate were observed; however, small areas of bone resorption were observed on the bone surface (Figure 3b).

Osteoclasts and resorption gaps were observed, close to areas of periosteum proliferation and formation of primary bone (Figure 3b). In bone defects filled with βTCP graft (TCP), hemorrhagic areas were observed close to the bone surface (Figure 3C). The particles of the βTCP graft within the granulation tissue presented areas of resorption (presence of osteoclasts) and areas of ossification near the bone surface (Figure 3e). In the TCP-LED bone defects, no areas of inflammatory infiltrate were observed. There were areas of bone resorption and areas of bone neoformation close to the periosteum (Figure 3d). There were βTCP particles close to areas of bone neoformation (Figure 3f), associated with areas of graft resorption similar to the TCP group.

14 days

After 14 d, primary bone tissue was observed at the edges of the bone defects associated with the periosteum (Figure 4). The center of the defects was filled by fibrous granulation tissue, with extensive vascularization. Areas of bone resorption and formation of primary bone spicules were observed in the Co and TCP bone defects (Figures 4a & 4b). In the Co-LED and TCP-LED bone defects, there were areas of bone neoformation close to the reminiscent bone at the edge of the defects. In the TCP-LED, βTCP particles close to the edge of the defect are surrounded by the primary bone (Figure 4d).

30 days

No group demonstrated complete ossification of the bone cavity at 30 d (Figure 5). Co and TCP bone defects showed bone spicules in the periphery of the bone defect (Figure 5a). In the TCP defects group, fibrosis and formation of foreign body giant cells were observed on the remaining graft particles in the central region of the defect (Figure 5c & 5e). On the other hand, irradiated defects (Co-LED and TCP-LED) presented primary bone formation along defect margins and no giant cells were presented around TCP particles (Figure 5d & 5f).

Discussion

The present study demonstrated that the use of βTCP associated with photobiomodulation accelerates the process of bone repair and remodeling. The association of the two treatments seems to have better effects on the remodeling of the bone defect edges, and organic and inorganic bone matrix synthesis. Besides, the blood clot appears to have been more quickly reabsorbed and replaced with granulation tissue, with no evidence of inflammatory reaction, in the groups treated with phototherapy on the 7th day. At 30 d, there was evidence of increased inorganic matrix deposition in the grafted and irradiated defects. Previous studies have demonstrated that the association of photobiomodulation with the βTCP graft can accelerate the deposition of collagen and hydroxyapatite matrix in regenerating bone tissue [17,24,25] or increase the volume of the mineralized matrix after three months [26]. However, the protocols used in these studies required a long period of treatment (every 48 h for two weeks), which could be inconvenient, requiring multiple patient return visits [17,24-26]. The photobiomodulation protocol used in the present study was initiated immediately after the surgical procedure and reapplied for 3 days, obtaining similar results. Besides, the dose used was lower (4.6 J/cm^2), requiring a shorter application time. The results obtained were similar to those reported by other authors, accelerating the process of bone repair and improving the quality of newly formed bone [17,18,24]. We scheduled to apply the photobiomodulation only up to the third day after surgery as the expression of genes associated with differentiation and proliferation of osteoblasts takes place in this period [18]. Moreover, the beginning of the bone formation process occurs on the third day [18]. The application of photobiomodulation in this period seems to accelerate the process of initial bone repair [18], corroborating the findings of the present study. Previous studies have demonstrated that photobiomodulation could be associated with increased proliferation of osteoprogenitor cells and differentiation of osteoblasts producing bone matrix, thus increasing the rate of bone neoformation and bone growth in the area of the defect [17,18]. An in vitro study demonstrated that a single session of red light (935nm) irradiation was able to increase the expression of osteoblast differentiation markers Runt-related transcription factor 2 (Runx-2), alkaline phosphatase, osteopontin, and increased the calcium deposits in human osteoblast cultures after 7 d [27]. So, longer periods of photobiomodulation treatment may not be necessary to improve initial bone repair. However, in large defects, the use of osteoinductive techniques alone might not provide enough bone repair. However, despite the stimulation of osteoblast differentiation by photobiomodulation, the use of grafts may be still necessary to act as an osteoconductive scaffold in critical-sized bone defects [17,24-26]. In the present study, the association of photobiomodulation with βTCP was demonstrated to be more efficient than the use of the therapies separately, even when applied only in the first 3 d of bone repair.

The anti-inflammatory and pro-healing effects of photobiomodulation [18,28,29] may have contributed to the reduction in the inflammatory reaction, removal of the blood clot, and filling of the bone defect with granulation tissue in the irradiated groups after 7 d. In the irradiated defects (Co-LED and TCP-LED), bone remodeling appears to have been initiated earlier, and at 7 d there were extensive areas of bone resorption on the margin of the defects. This reaction was also observed in the non-irradiated defects (Co and TCP) but after 14 d. This suggests that bone tissue damaged in the surgical procedure was reabsorbed more rapidly after photobiomodulation. Indeed, experimental studies have shown that irradiation of bone tissue promotes bone remodeling, with activation of osteoblasts and osteoclasts [28,30]. The βTCP may promote some undesirable reactions during the process of bone regeneration, such as the formation of fibrosis, chronic inflammation, and multinucleated giant cell/foreign body reactions, and not reconstitute the entire bone volume [3,11-13]. In the present study, foreign body reactions and fibrosis were observed in the TCP group after 30 d. However, the TCP-LED group did not present a foreign body reaction, suggesting that phototherapy may stimulate bone matrix synthesis and remodeling of βTCP graft particles, inhibiting the formation of tissue fibrosis. The formation of multinucleated giant cells and fibrosis was observed around biomaterials inserted in soft tissues and bone grafts and is associated with the activation and recruitment of macrophages in the initial stages of the inflammatory process [31-33]. However, the use of anti-inflammatory agents can reduce fibrosis and multinucleated giant cell formation [34,35]. A study demonstrated that photobiomodulation could inhibit the acute inflammatory reaction and blunt foreign body reactions in an experimental model of osteoarthritis [36]. The anti-inflammatory properties of photobiomodulation include driving differentiation of macrophages towards M2 (anti-inflammatory phenotype), a decrease of M1 recruitment, and inhibition of production of cytokines regulating foreign body reactions, such as tumor necrosis factor-alpha and interferon-gamma [29,37-40]. As observed in the present study, inflammatory cell infiltration was absent in the Co-LED and TCP-LED after 7 days. So the absence of inflammatory cell migration might be accounted for the inhibition of foreign body reaction in TCP-LED defects.

Conclusion

We conclude that phototherapy applied in the first three days after βTCP grafting accelerates the initial bone repair and deposition of the inorganic matrix in bone defects, reducing initial inflammatory infiltration, and avoiding foreign body reactions. The association of βTCP grafts with phototherapy presents better effects on initial tissue repair than isolated treatments.

Acknowledgment

This work was supported by the Coordination for the Improvement of Higher Education Personnel (CAPES) (granting a scholarship to C.P.S., grant n. 06172286986/2015) and by Fundação Araucária – PR, (granting a scholarship to R.P.G, n.174/2015).

References

1. Gorla LF, Spin NR, Boos FB, Pereira RS, Garcia IR, et al. (2015) Use of autogenous bone and beta-tricalcium phosphate in maxillary sinus lifting: a prospective, randomized, volumetric computed tomography study. International journal of oral and maxillofacial surgery 44(12): 1486-1491.

2. Jelusic D, Zirk ML, Fienitz T, Plancak D, Puhar I, et al. (2016) Monophasic ss-TCP vs. biphasic HA/ss-TCP in two-stage sinus floor augmentation procedures - a prospective randomized clinical trial. Clinical oral implants research 28(10): 175-183.

3. Naineni R, Ravi V, Subbaraya DK, Prasanna JS, Panthula VR, et a. (2016) Effect of Alendronate with beta - TCP Bone Substitute in Surgical Therapy of Periodontal Intra-Osseous Defects: A Randomized Controlled Clinical Trial. Journal of clinical and diagnostic research : JCDR 10(8): ZC113-117.

4. Stiller M, Kluk E, Bohner M, Lopez MA, Muller MC, et al. (2014) Performance of beta-tricalcium phosphate granules and putty, bone grafting materials after bilateral sinus floor augmentation in humans. Biomaterials 35(10): 3154-3163.

5. Trombelli L, Franceschetti G, Stacchi C, Minenna L, Riccardi O, et al. (2014) Minimally invasive transcrestal sinus floor elevation with deproteinized bovine bone or beta-tricalcium phosphate: a multicenter, double-blind, randomized, controlled clinical trial. Journal of clinical periodontology 41(3): 311-319.

6. Weibull L, Widmark G, Ivanoff CJ, Borg E, Rasmusson L (2009) Morbidity after chin bone harvesting--a retrospective long-term follow-up study. Clinical implant dentistry and related research 11(2): 149-157.

7. Cordaro L, Torsello F, Miuccio MT, di Torresanto VM, Eliopoulos D (2011) Mandibular bone harvesting for alveolar reconstruction and implant placement: subjective and objective cross-sectional evaluation of donor and recipient site up to 4 years. Clinical oral implants research 22(11): 1320-1326.

8. Janssen NG, Schreurs R, de Ruiter AP, Sylvester-Jensen HC, Blindheim G, et al. (2019) Microstructured beta-tricalcium phosphate for alveolar cleft repair: a two-centre study. International journal of oral and maxillofacial surgery 48(6): 708-711.

9. Pereira RS, Gorla LF, Boos F, Okamoto R, Garcia Junior IR, et al. (2017) Use of autogenous bone and beta-tricalcium phosphate in maxillary sinus lifting: histomorphometric study and immunohistochemical assessment of RUNX2 and VEGF. International journal of oral and maxillofacial surgery 46(4): 503-510.

10. Prins HJ, Schulten EA, Ten Bruggenkate CM, Klein-Nulend J, Helder MN (2016) Bone Regeneration Using the Freshly Isolated Autologous Stromal Vascular Fraction of Adipose Tissue in Combination With Calcium Phosphate Ceramics. Stem cells translational medicine 5(10): 1362-1374.

11. Hirota M, Matsui Y, Mizuki N, Kishi T, Watanuki K, et al. (2009) Combination with allogenic bone reduces early absorption of beta-tricalcium phosphate (beta-TCP) and enhances the role as a bone regeneration scaffold. Experimental animal study in rat mandibular bone defects. Dental materials journal 28(2): 153-161.

12. Bizenjima T, Takeuchi T, Seshima F, Saito A (2016) Effect of poly (lactide-co-glycolide) (PLGA)-coated beta-tricalcium phosphate on the healing of rat calvarial bone defects: a comparative study with pure-phase beta-tricalcium phosphate. Clinical oral implants research 27(11): 1360-1367.

13. Devi R, Dixit J (2016) Clinical Evaluation of Insulin like Growth Factor-I and Vascular Endothelial Growth Factor with Alloplastic Bone Graft Material in the Management of Human Two Wall Intra-Osseous Defects. Journal of clinical and diagnostic research : JCDR 10(9): ZC41-ZC46.

14. Martinez A, Balboa O, Gasamans I, Otero XL, Guitian F (2015) Deproteinated bovine bone vs. beta-tricalcium phosphate as bone graft substitutes: histomorphometric longitudinal study in the rabbit cranial vault. Clinical oral implants research 26(6): 623-632.

15. Chung SM, Jung IK, Yoon BH, Choi BR, Kim DM, et al. (2016) Evaluation of Different Combinations of Biphasic Calcium Phosphate and Growth Factors for Bone Formation in Calvarial Defects in a Rabbit Model. The International journal of periodontics & restorative dentistry 36 Suppl: s49-59.

16. Tian Y, Lu T, He F, Xu Y, Shi H, et al. (2018) Beta-tricalcium phosphate composite ceramics with high compressive strength, enhanced osteogenesis and inhibited osteoclastic activities. Colloids Surf B Biointerfaces 167: 318-327.

17. Pinheiro AL, Soares LG, Aciole GT, Correia NA, Barbosa AF, et al. (2011) Light microscopic description of the effects of laser phototherapy on bone defects grafted with mineral trioxide aggregate, bone morphogenetic proteins, and guided bone regeneration in a rodent model. Journal of biomedical materials research Part A 98(2): 212-221.

18. Tim CR, Bossini PS, Kido HW, Malavazi I, von Zeska Kress MR, et al. (2016) Effects of low level laser therapy on inflammatory and angiogenic gene expression during the process of bone healing: A microarray analysis. Journal of photochemistry and photobiology B, Biology 154: 8-15.

19. Batista JD, Sargenti NS, Dechichi P, Rocha FS, Pagnoncelli RM (2015) Low-level laser therapy on bone repair: is there any effect outside the irradiated field? Lasers in medical science 30(5): 1569-1574.

20. Romao MM, Marques MM, Cortes AR, Horliana AC, Moreira MS, et al. (2015) Micro-computed tomography and histomorphometric analysis of human alveolar bone repair induced by laser phototherapy: a pilot study. International journal of oral and maxillofacial surgery 44(12): 1521-1528.

21. AboElsaad NS, Soory M, Gadalla LM, Ragab LI, Dunne S, et al. (2009) Effect of soft laser and bioactive glass on bone regeneration in the treatment of bone defects (an experimental study). Lasers in medical science 24(4): 527-533.

22. Park CH, Abramson ZR, Taba M, Jin Q, Chang J, et al. (2007) Three-dimensional micro-computed tomographic imaging of alveolar bone in experimental bone loss or repair. Journal of periodontology 78(2): 273-281.

23. Sawyer AA, Song SJ, Susanto E, Chuan P, Lam CX, et al. (2009) The stimulation of healing within a rat calvarial defect by mPCL-TCP/collagen scaffolds loaded with rhBMP-2. Biomaterials 30(13): 2479-2488.

24. Pinheiro AL, Soares LG, Marques AM, Aciole JM, de Souza RA, et al. (2014) Raman ratios on the repair of grafted surgical bone defects irradiated or not with laser (lambda780 nm) or LED (lambda850 nm). Journal of photochemistry and photobiology B, Biology 138:146-154.

25. Soares LG, Marques AM, Guarda MG, Aciole JM, dos Santos JN, et al. (2014) Influence of the lambda780nm laser light on the repair of surgical bone defects grafted or not with biphasic synthetic micro-granular hydroxylapatite+Beta-Calcium triphosphate. Journal of photochemistry and photobiology B, Biology 131: 16-23.

26. Oliveira G, Aroni MAT, Medeiros MC, Marcantonio E, Marcantonio RAC (2018) Effect of low-level laser therapy on the healing of sites grafted with coagulum, deproteinized bovine bone, and biphasic ceramic made of hydroxyapatite and beta-tricalcium phosphate. In vivo study in rats. Lasers Surg Med.

27. Tani A, Chellini F, Giannelli M, Nosi D, Zecchi OS, et al. (2018) Red (635 nm), Near-Infrared (808 nm) and Violet-Blue (405 nm) Photobiomodulation Potentiality on Human Osteoblasts and Mesenchymal Stromal Cells: A Morphological and Molecular In Vitro Study. Int J Mol Sci 19(7).

28. Maia LG, Alves AV, Bastos TS, Moromizato LS, Lima IB, et al. (2014) Histological analysis of the periodontal ligament and alveolar bone during dental movement in diabetic rats subjected to low-level laser therapy. Journal of photochemistry and photobiology B, Biology 135: 65-74.

29. Hamblin MR (2017) Mechanisms and applications of the anti-inflammatory effects of photobiomodulation. AIMS Biophys 4(3): 337-361.

30. Altan BA, Sokucu O, Ozkut MM, Inan S (2012) Metrical and histological investigation of the effects of low-level laser therapy on orthodontic tooth movement. Lasers in medical science 27(1): 131-140.

31. Malik AF, Hoque R, Ouyang X, Ghani A, Hong E, et al. (2011) Inflammasome components Asc and caspase-1 mediate biomaterial-induced inflammation and foreign body response. Proceedings of the National Academy of Sciences of the United States of America 108(50): 20095-20100.

32. Moore LB, Sawyer AJ, Charokopos A, Skokos EA, Kyriakides TR (2015) Loss of monocyte chemoattractant protein-1 alters macrophage polarization and reduces NFkappaB activation in the foreign body response. Acta biomaterialia 11: 37-47.

33. Miron RJ, Zohdi H, Fujioka KM, Bosshardt DD (2016) Giant cells around bone biomaterials: Osteoclasts or multi-nucleated giant cells? Acta biomaterialia 46: 15-28.

34. Kastellorizios M, Tipnis N, Burgess DJ (2015) Foreign Body Reaction to Subcutaneous Implants. Advances in experimental medicine and biology 865: 93-108.

35. Morais JM, Papadimitrakopoulos F, Burgess DJ (2010) Biomaterials/tissue interactions: possible solutions to overcome foreign body response. The AAPS journal 12(2): 188-196.

36. Rubio CR, Cremonezzi D, Moya M, Soriano F, Palma J, et al. (2010) Helium-neon laser reduces the inflammatory process of arthritis. Photomed Laser Surg 28(1): 125-129.

37. Vollkommer T, Henningsen A, Friedrich RE, Felthaus OH, Eder F, et al. (2019) Extent of Inflammation and Foreign Body Reaction to Porous Polyethylene In Vitro and In Vivo. In Vivo 33(2): 337-347.

38. Fernandes KP, Souza NH, Mesquita RA, Silva Dde F, Rocha LA, et al. (2015) Photobiomodulation with 660-nm and 780-nm laser on activated J774 macrophage-like cells: Effect on M1 inflammatory markers. Journal of photochemistry and photobiology B, Biology 153: 344-351.

39. Fukuda TY, Tanji MM, Silva SR, Sato MN, Plapler H (2013) Infrared low-level diode laser on inflammatory process modulation in mice: pro- and anti-inflammatory cytokines. Lasers in medical science 28(5): 1305-1313.

40. Cassini VP, de Carvalho, da Silva RF, Russo RC, Araujo FA, et al. (2018) Lack of interferon-gamma attenuates foreign body reaction to subcutaneous implants in mice. Journal of biomedical materials research Part A 106(8): 2243-2250.